THZ TRANSMISSION SPECTROSCOPY APPLIED TO DIELECTRICS AND MICROWAVE CERAMICS

ALEXEJ PASHKIN, ELENA BUIXADERAS, PETR KUŽEL
Institute of Physics, Academy of Science of Czech Republic,
Na Slovance 2, 18221 Prague 8, Czech Republic

MEI-HUI LIANG, CHEN-TI HU, I-NAN LIN
Materials Science Center, National Tsing-Hua University, 101 Kuang-Fu rd., Hsinchu, Taiwan, R. O. C.

The room-temperature complex dielectric function of $Ba(Mg_{1/3}Ta_{2/3})O_3$ (BMT) high-permittivity microwave ceramics was measured in the sub-millimeter spectral range using the time-domain terahertz-transmission spectroscopy. The capabilities of the method and unambiguous evaluation of the dielectric function are also discussed.

INTRODUCTION

The method of time-domain terahertz-transmission spectroscopy (TDTTS) has been developed in recent ten years due to the appearance of self-modelocked lasers that generate light in form of extremely short femtosecond pulses. It gave possibility to emit sub-picosecond THz pulses[1-7] (i.e. ultra-broadband electromagnetic transients with a central frequency near 1 THz). Correspondingly, the detection techniques which allow measurements of the THz pulse time profile were also discovered[8-11]. The spectral range covered by TDTTS constitutes a bridge between the classical IR spectroscopy domain and
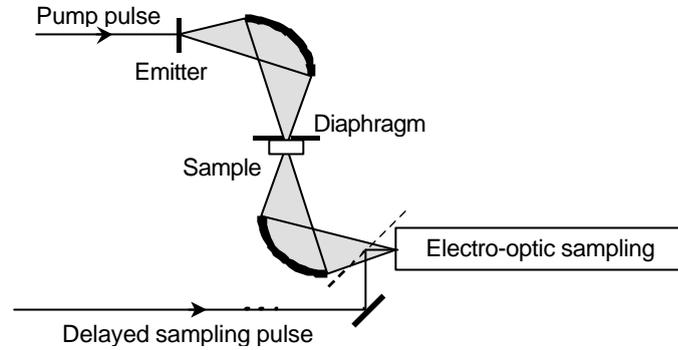
FIGURE 1 Scheme of the TDTTS experiment.

the frequencies accessible by microwave techniques [12]. The TDTTS method was shown to be useful for the study of polar excitations as well as in gases and liquids[13], as in solids like semiconductors, superconductors, and dielectrics[12].

In this contribution we describe our experimental setup and discuss the determination of the complex dielectric spectra. The room temperature transmission measurements of the BMT ceramics are presented. We compare them to the previously published results obtained by other techniques and briefly discuss the observed differences.

EXPERIMENTAL SETUP AND PRINCIPLE OF THE METHOD

Our experimental setup (see Figure 1) uses a Lexel 480 Ti:sapphire laser oscillator (80 fs, 800 nm) as the light source. Horizontally polarized THz pulses were generated in biased large-aperture photoconducting antennas made of low-temperature grown GaAs. The electro-optic sampling technique[14] with a 1 mm thick high-resistivity <110> ZnTe sensor crystal was employed for the phase sensitive detection of the pulses. The dynamic range of the measurements was better than 10^3. Typical spectral resolution of the system is 0.5 cm^{-1}.

The above described detection system allows to measure of the time profile of the electric field of the THz pulses. The spectroscopic method consists in the measurement of a reference waveform $E_r(t)$

with an empty diaphragm and a signal waveform $E_s(t)$ with the sample attached to the diaphragm and filling the whole aperture. The Fourier components of the two signals are obtained through the fast Fourier transform and they define the complex transmission function of the sample:

$$t(\omega) = E_s(\omega)/E_r(\omega). \tag{1}$$

In the case of a homogeneous sample the complex refraction index $N = n + i\kappa$ is related to the complex transmission through

$$t(\omega) = \frac{4N \exp[i\omega(N-1)d/c]}{(N+1)^2} \sum_{k=0}^{m} \left[\left(\frac{N-1}{N+1} \right) \exp(i\omega N d/c) \right]^{2k}, \tag{2}$$

where d is the sample thickness, c is the light velocity and m is the number of reflections in the sample. These reflections are experimentally resolved (at least for thick samples) and form separate pulses in the measured signal so that the value of the coefficient m can be easily determined.

Equation (2) constitutes two real equations for two real parameters n and κ: e.g., for $m = 0$ the expressions for the modulus $|t|$ and the phase φ of the transmission function take the form:

$$|t| = \frac{2\sqrt{n^2 + \kappa^2}}{(n+1)^2 + \kappa^2} \exp(-\omega\kappa d/c) \tag{3a}$$

$$\varphi + 2\pi l = \omega(n-1)d/c + \arctan\left(-\kappa \frac{n^2 + \kappa^2 - 1}{n(n+1)^2 + \kappa^2(n+1)} \right) \tag{3b}$$

The first right-hand side term of equation (3b) accounts for the decrease of the phase velocity during the propagation in the sample; the second one, which constitutes usually only a small correction, describes the phase change on the interfaces. The phase φ is defined by the Fourier transform of the experimental data and ranges from 0 to

2π; the term $2\pi l$ is added to obtain the right order of the phase displacement. The integer parameter l can be determined for the peak frequency of the transmitted spectrum from the measured time delay between the signal and the reference pulses $[t = (n-1)d/c]$. The equations can then be solved numerically for n and κ. The same reflection is in principle valid for $m \neq 0$: one obtains slightly more complicated expressions analogic to (3a,b) which can be solved numerically.

The situation becomes more complicated when the sample's THz spectrum contains a very sharp dielectric resonance or a narrow strongly absorbing spectral band. The difficulty then comes from the fact that, due to the low spectral resolution or due to the weakness of the signal, it is not immediately clear how many orders of the phase are swept near the resonant frequency (i.e. what is the strength of the related dielectric anomaly). As TDTTS allows to access independently both the real and the imaginary part of the dielectric function, which, in turn, should satisfy the Kramers-Kronig (KK) relations[15], it is then possible to use these relations to leave the remaining ambiguity. As an illustration of this procedure we studied the case of the lithium germanate $Li_2Ge_7O_{15}$ (LGO), which presents a sharp low-frequency
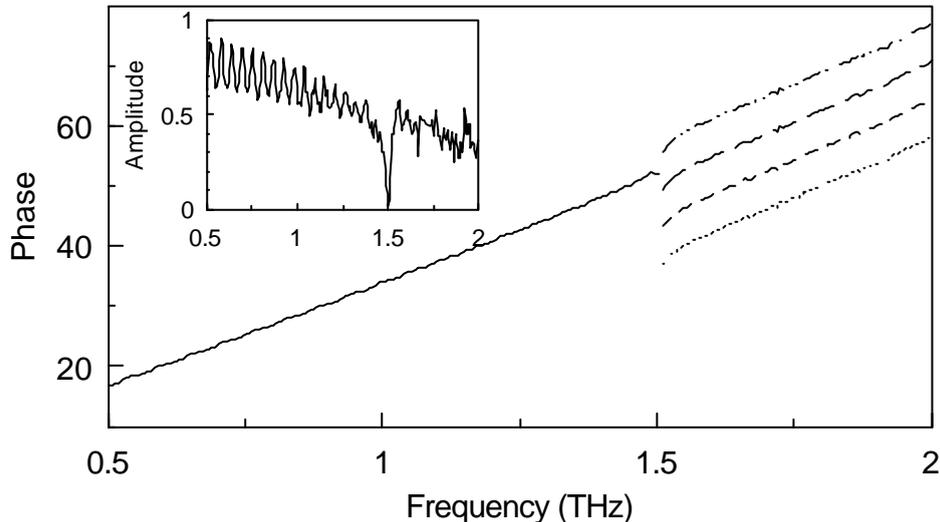
FIGURE 2 Complex transmission function of a 0.98 mm thick LGO sample; see text for details.

phonon at about 1.5 THz for the propagation along its polar *c* axis[15].

The transmission function of a LGO sample is shown in Figure 2. The interference fringes of the amplitude are due to the sample internal reflections ($m = 2$). The values of the phase displacement for the frequencies below the phonon resonance are determined from the measured time delay between the reference and signal pulses; the correct phase branch at high frequencies needs to be determined through the KK analysis. Couples of possible n and κ coming from different branches can be determined through equation (2). However, only the true n and κ should satisfy the KK relations. The results of KK analysis for LGO are shown in Figure 3 (only the results related to the two dashed curves in Figure 2 were represented here). In Figure 3a the strength of the resonance obtained by the direct solution of equation (2) is in a good agreement with the strength obtained indirectly from κ through the KK analysis. Thus, Figure 3a is obtained from the correct phase branch while the values in Figure 3b come from a wrong one. As the KK relations have integral character one cannot expect to obtain an agreement for the slow continuous increase of n (see Figure 3a) which is clearly related to the higher-frequency
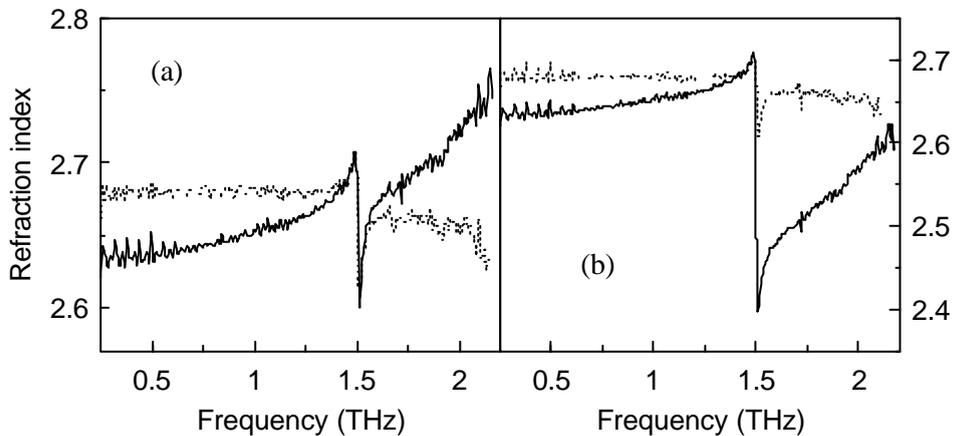
FIGURE 3 Refraction index of LGO. Solid lines: n calculated from transmission function using equation (2); dotted lines: n calculated from κ through KK relations. Phase branch choice following the notation of Figure 2: (a) long-dashed line, (b) short-dashed line.

phonons and thus cannot be accounted for correctly within the KK analysis of our data.

EXPERIMENTAL RESULTS AND DISCUSSION

$Ba(Mg_{1/3}Ta_{2/3})O_3$ ceramics have been intensively investigated during the last years because of its low microwave dielectric losses. This feature makes it very attractive for applications. The dielectric properties of BMT ceramics have been studied so far by means of infrared and microwave spectroscopy[16-18]. It was found that the losses depend on technology of preparation[19]. An existence of a second non-perovskite phase or other defects can essentially decrease the dielectric quality factor: we have applied TDTTS method to the investigation of this effect in the sub-millimeter spectral region.

The studied samples can be divided into three groups according to the technology of preparation. First group consisted of samples prepared by usual mixed oxide technology. This method is realized through the reaction between magnesium and tantalum oxides and barium carbonate ($BaCO_3+MgO+Ta_2O_3$). Second group was also prepared by the mixed oxide technology, in addition, $BaZrO_3$ was added into the mixture in the ratio of 2 mol % providing a zirconium doped BMT. The third group consisted of BMT samples obtained as a product of the reaction between alkoxides

$$Ba\,(OR_1)_2 + Mg\,(OR_2)_2 + Ta\,(OR_3)_5,$$
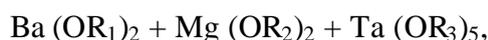
where R is an alcoholic radical such as C_2H_5O or similar.

Each group included samples with several sintering temperatures of ceramics from 1450°C to 1600°C (four samples per group). Samples were prepared in the form of plane parallel pellets with the diameter of 6 mm and the thickness of 0.2–0.25 mm.

Measurements showed that sintering temperature has no essential influence on the sub-millimeter dielectric spectra of BMT ceramics. Small observed changes in the permittivity (few per cent) are not probably related with this technological parameter. Therefore for detailed investigation have been chosen one sample from each group

which had better characteristics (1500 °C sintered alkoxide and mixed
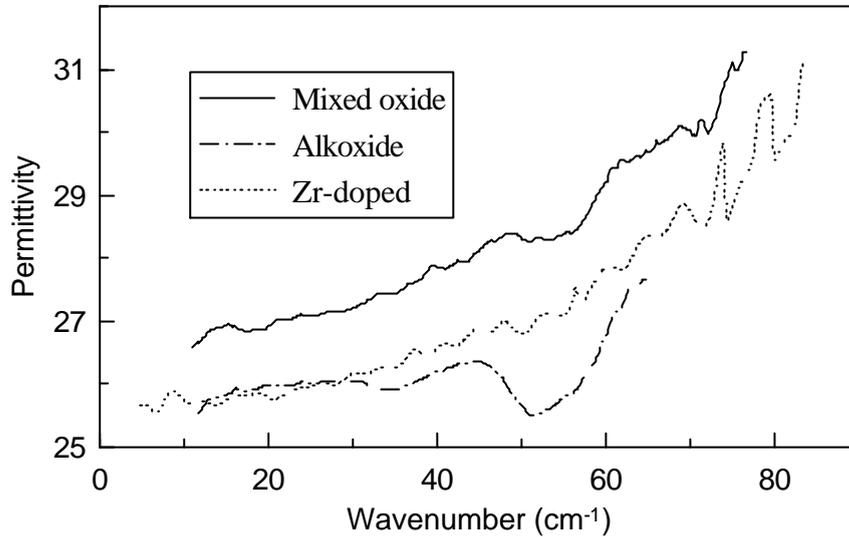
FIGURE 4   Permittivity of BMT ceramics obtained by TDTTS.
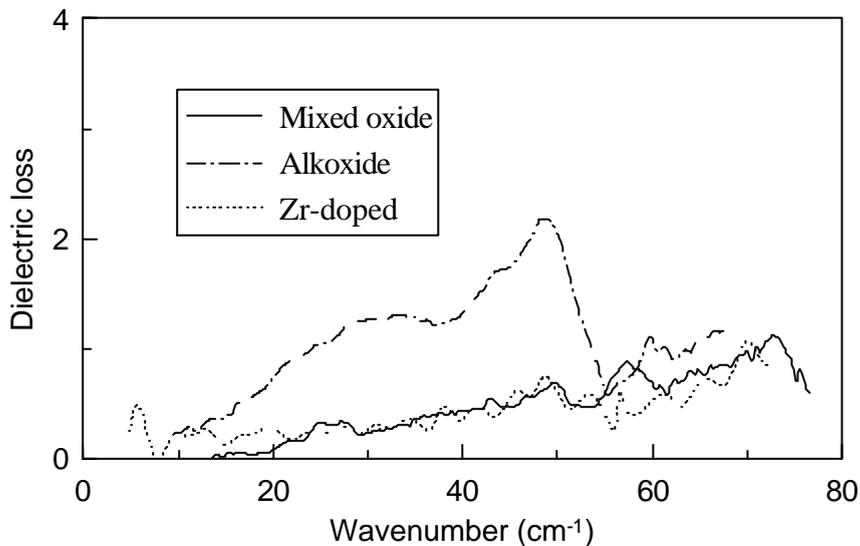
FIGURE 5   Dielectric losses of BMT ceramics obtained by TDTTS.

oxide samples and 1550 °C sintered Zr-doped sample). Their dielectric spectra are shown in Figures 4 and 5.

Our data are in agreement with the data obtained by other techniques in lower and higher frequency range[16,17,18]: the continuous increase of the permittivity is due to a phonon resonance at 138 cm^{-1} [16]. For

alkoxide BMT samples we observe an additional resonances in the range of 30–60 cm^{-1}. Since the other samples do not present this feature one can conclude that it is related to the traces of second non-perovskite phase of unknown structure.

References
[1] D. H. Auston, and M. C. Nuss, <u>IEEE J. Quantum Electron.</u>, **24**, 184 (1988).
[2] X.-C. Zhang, X. F. Ma, Y. Jin, T.-M. Lu, E. P. Boden, D. P. Phelps, K. R. Stewart, and C. P. Yakymyshyn, <u>Appl. Phys. Lett.</u>, **61**, 3080 (1993).
[3] P. R. Smith, D. H. Auston, and M. C. Nuss, <u>IEEE J. Quantum Electron.</u>, **24**, 255 (1988).
[4] C. H. Fattinger, and D. Grischkowsky, <u>Appl. Phys. Lett.</u>, **54**, 490 (1989).
[5] B. B. Hu, J. T. Darrow, X.-C. Zhang, D. H. Auston, and P. R. Smith, <u>Appl. Phys. Lett.</u>, **56**, 886 (1990).
[6] J. T. Darrow, B. B. Hu, X.-C. Zhang, and D. H. Auston, <u>Opt. Lett.</u>, **15**, 323 (1990).
[7] X.-C. Zhang, B. B. Hu, J. T. Darrow, and D. H. Auston, <u>Appl. Phys. Lett.</u>, **56**, 1011 (1990).
[8] Ch. Fattinger, and D. Grischkowsky, <u>Appl. Phys. Lett.</u>, **53**, 1480 (1988).
[9] D. H. Auston, K. P. Cheung, and P. R. Smith, <u>Appl. Phys. Lett.</u>, **45**, 284 (1984).
[10] D. H. Auston, K. P. Cheung, J. A. Valdmanis, and D. A. Kleinman, <u>Phys. Rev. Lett.</u>, **53**, 1555 (1984).
[11] Q. Wu, M. Litz, and X.-C. Zhang, <u>Appl. Phys. Lett.</u>, **68**, 2924 (1996).
[12] G. Grüner (ed.), <u>Millimeter and Submillimeter Wave Spectroscopy of Solids</u>, Chap. 2, p. 7 (Springer-Verlag Berlin Heidelberg, 1998).
[13] M. van Exter, Ch. Fattinger, and D. Grishkowsky, <u>Opt. Lett.</u>, **14**, 1128 (1989).
[14] Q. Wu, and X.-C. Zhang, <u>Appl. Phys. Lett.</u>, **68**, 1604 (1996).
[15] C. F. Klingshirn, <u>Semiconductor Optics</u>, Chap. 8, p. 92 (Springer-Verlag Berlin Heidelberg, 1995).
[16] F. Kadlec, J. Petzelt, V. Železný, and A. A. Volkov, <u>Solid State Commun.</u>, **94**, 725 (1995).
[17] Djuniadi A. Sagala and Shigeji Koyasu, <u>J. Am. Ceram. Soc.</u>, **76**, 2433-36 (1993).
[18] J. Petzelt, and N. Setter, <u>Ferroelectrics</u>, **150**, 89-102 (1993).
[19] J. Petzelt, S. Kamba, G. V. Kozlov, and A. A. Volkov, <u>Ferroelectrics</u>, **176**, 145-165 (1996).
[20] S. Kamba, J. Petzelt, R. Freer et al. <u>Proc. Electronic ceramics & Appl.</u>, p. 63-66 Aveiro 1996

THZ SPECTROSCOPY APPLIED TO MICROWAVE CERAMICS